University of Texas Rio Grande Valley

ScholarWorks @ UTRGV

3-2024

Evaluation of Exploratory Fluid Biomarker Results from a Phase 1 Senolytic Trial in Mild Alzheimer's Disease

Miranda E. Orr

Valentina R. Garbarino
University of Texas Health Science Center at San Antonio

Juan Pablo Palavicini
University of Texas Health Science Center at San Antonio

Justin Melendez
University of Texas Health Science Center at San Antonio

Nicolas Barthelemy
University of Texas Health Science Center at San Antonio

See next page for additional authors

Follow this and additional works at: https://scholarworks.utrgv.edu/som_pub

Part of the Medicine and Health Sciences Commons

Authors

Miranda E. Orr, Valentina R. Garbarino, Juan Pablo Palavicini, Justin Melendez, Nicolas Barthelemy, Yingxin He, Tiffany F. Kautz, Marisa Lopez-Cruzan, Julia Mathews, Peng Xu, and Bin Zhan

Evaluation of Exploratory Fluid Biomarker Results from a Phase 1 Senolytic Trial in Mild Alzheimer's Disease

Miranda Orr

morr@wakehealth.edu

Wake Forest School of Medicine   https://orcid.org/0000-0002-0418-2724

Valentina Garbarino
University of Texas Health Science Center

Juan Palavicini
University of Texas Health Science Center   https://orcid.org/0000-0001-9667-8438

Justin Melendez
Washington University   https://orcid.org/0000-0003-3629-3274

Nicolas Barthélemy
Washington University School of Medicine   https://orcid.org/0000-0003-4937-2860

Yingxin He
Washington University School of Medicine   https://orcid.org/0000-0003-2543-4553

Tiffany Kautz
University of Texas Health Science Center

Marisa Lopez-Cruzan
University of Texas Health Science Center

Julia Mathews
University of Texas Health Science Center

Peng Xu
Icahn School of Medicine at Mount Sinai   https://orcid.org/0000-0001-8007-9879

Bin Zhang
Icahn School of Medicine at Mount Sinai

Afaf Saliba
University of Texas Health Science Center   https://orcid.org/0000-0003-2576-4069

Nagarjunachary Ragi
University of Texas Health Science Center

Kumar Sharma
University of Texas Health Science Center

Suzanne Craft

Wake Forest School of Medicine

Ronald (C.) Petersen

Mayo Clinic   https://orcid.org/0000-0002-8178-6601

Jair Espindola-Netto

Mayo Clinic

Ailing Xue

Mayo Clinic

Tamara Tchkonia

Mayo Clinic

James Kirkland

https://orcid.org/0000-0003-1676-4905

Sudha Seshadri

University of Texas Health Science Center   https://orcid.org/0000-0001-6135-2622

Arash Salardini

University of Texas Health Science Center

Nicolas Musi

UTHSC San Antonio

Randall Bateman

Washington University in St. Louis   https://orcid.org/0000-0002-7729-1702

Mitzi Gonzales

Cedars Sinai Medical Center

Article

Keywords:

Additional Declarations: Yes there is potential Competing Interest. R.C.P. receives royalties from Oxford University Press and UpToDate and receives fees from Medscape for educational activities. J.L.K. and T.T. are co-investigators on a patent for Killing Senescent Cells and Treating Senescence-Associated Conditions Using an SRC Inhibitor and a Flavonoid and a patent for Treating Cognitive Decline and Other Neurodegenerative Conditions by Selectively Removing Senescent Cells from Neurological Tissue that are held by Mayo Clinic with royalties paid to Mayo Clinic by Unity Biotechnologies. S.C. reports Scientific Advisory Board membership for T3D Therapeutics and the Neurodegenerative Consortium, and reports

Evaluation of Exploratory Fluid Biomarker Results from a Phase 1 Senolytic Trial in Mild Alzheimer's Disease

Valentina R. Garbarino, PhD[1,2], Juan Pablo Palavicini, PhD[3,4], Justin Melendez, PhD[5,6], Nicolas Barthelemy, PhD[5,6], Yingxin He, PhD[5,6], Tiffany F. Kautz, PhD[1,3], Marisa Lopez-Cruzan, PhD[4,7], Julia J. Mathews, BS[1], Peng Xu, PhD[8,9], Bin Zhang, PhD[8,9], Afaf Saliba[10], Nagarjunachary Ragi[10], Kumar Sharma[10], Suzanne Craft, PhD[11], Ronald C. Petersen, MD[12], Jair Machado Espindola-Netto, PhD[13], Ailing Xue, PhD[13], Tamara Tchkonia, PhD[13], James L. Kirkland, MD, PhD[14], Sudha Seshadri, MD[1,15,16], Arash Salardini, MD[1,15], Nicolas Musi, MD[17], Randall J. Bateman, MD[5,6], Mitzi M. Gonzales, PhD*[1,18], Miranda E. Orr, PhD*[11,19]

[1]Glenn Biggs Institute for Alzheimer's & Neurodegenerative Diseases, University of Texas Health Science Center at San Antonio, San Antonio, TX, USA

[2]Department of Cell Systems and Anatomy, University of Texas Health Science Center at San Antonio, San Antonio, TX, USA

[3]Department of Medicine, University of Texas Health Science Center at San Antonio, San Antonio, TX, USA

[4]Barshop Institute for Longevity and Aging Studies, University of Texas Health San Antonio, San Antonio, TX, USA

[5]Department of Neurology, Washington University School of Medicine, St. Louis, MO, USA

[6]Tracy Family SILQ Center for Neurodegenerative Biology, St. Louis, MO, USA

[7]Department of Psychiatry, University of Texas Health Science Center at San Antonio, San Antonio, TX, USA

[8]Department of Genetics and Genomic Sciences, Icahn School of Medicine at Mount Sinai, New York, NY, USA

26   [9]Mount Sinai Center for Transformative Disease Modeling, Icahn School of Medicine at Mount

27   Sinai, New York, NY, USA

28   [10]Center for Precision Medicine, University of Texas Health Science Center at San Antonio, San

29   Antonio, TX, USA

30   [11]Department of Internal Medicine Section on Gerontology and Geriatric Medicine, Wake Forest

31   School of Medicine, Winston-Salem, NC, USA

32   [12]Department of Neurology, Mayo Clinic, Rochester, MN, USA

33   [13]Department of Physiology and Biomedical Engineering, Mayo Clinic, Rochester, MN, USA

34   [14]Department of Internal Medicine, Mayo Clinic, Rochester, MN, USA

35   [15]Department of Neurology, University of Texas Health Science Center at San Antonio, San

36   Antonio, TX, USA

37   [16]Department of Neurology, Boston University School of Medicine, Boston, MA, USA

38   [17]Department of Medicine, Cedars-Sinai Medical Center, Los Angeles, CA, USA

39   [18]Department of Neurology, Cedars Sinai Medical Center, Los Angeles, CA, USA

40   [19]Salisbury VA Medical Center, Salisbury, NC, 28144, USA

41

42   ***Co-Corresponding Author**

Miranda E. Orr	Mitzi M. Gonzales
575 Patterson Ave	8700 Beverly Blvd
Winston-Salem, NC 27101	Los Angeles, CA 90048
(336)716-7804	(424) 315-0228
morr@wakehealth.edu	mitzi.gonzales@cshs.org

43

44

45

Abstract

Senescent cell accumulation contributes to the progression of age-related disorders including Alzheimer's disease (AD). Clinical trials evaluating senolytics, drugs that clear senescent cells, are underway, but lack standardized outcome measures. Our team recently published data from the first open-label trial to evaluate senolytics (dasatinib plus quercetin) in AD. After 12-weeks of intermittent treatment, we reported brain exposure to dasatinib, favorable safety and tolerability, and modest post-treatment changes in cerebrospinal fluid (CSF) inflammatory and AD biomarkers using commercially available assays. Herein, we present more comprehensive exploratory analyses of senolytic associated changes in AD relevant proteins, metabolites, lipids, and transcripts measured across blood, CSF, and urine. These analyses included mass spectrometry for precise quantification of amyloid beta (Aß) and tau in CSF; immunoassays to assess senescence associated secretory factors in plasma, CSF, and urine; mass spectrometry analysis of urinary metabolites and lipids in blood and CSF; and transcriptomic analyses relevant to chronic stress measured in peripheral blood cells. Levels of Aß and tau species remained stable. Targeted cytokine and chemokine analyses revealed treatment-associated increases in inflammatory plasma fractalkine and MMP-7 and CSF IL-6. Urinary metabolites remained unchanged. Modest treatment-associated lipid profile changes suggestive of decreased inflammation were observed both peripherally and centrally. Blood transcriptomic analysis indicated downregulation of inflammatory genes including *FOS, FOSB, IL1β, IL8, JUN, JUNB, PTGS2*. These data provide a foundation for developing standardized outcome measures across senolytic studies and indicate distinct biofluid-specific signatures that will require validation in future studies.

ClinicalTrials.gov: NCT04063124.

Introduction

Senescent cell accumulation and the resultant pro-inflammatory senescence associated secretory phenotype (SASP) have been linked with the amyloid ß (Aß) and tau pathologies of Alzheimer's disease and related dementias (AD; ADRDs)[1-3]. In light of this, senescent cell clearance is being explored as a novel therapeutic mechanism for AD (for review:[4,5]; ongoing trials: SToMP-AD: NCT04685590, ALSENLITE: NCT04785300; STAMINA: NCT05422885). Targeted removal of senescent cells with the senolytic therapy that has been most comprehensively characterized and studied, combined dasatinib plus quercetin (D+Q), has demonstrated successful reduction of AD-related neuropathological burden of tau-containing neurofibrillary tangles (NFTs)[1] and Aß plaques[3], and prevented age-associated cognitive deficits in animal models[6,7]. We previously reported the outcomes of a 12-week open-label pilot study (Senolytic Therapy to Modulate the Progression of AD: SToMP-AD; NCT04063124), aimed at determining blood-brain barrier penetrance and safety and tolerability of D+Q in five study participants with early-stage symptomatic AD[8]. D but not Q, was detectable in the cerebrospinal fluid (CSF), and the intervention was well-tolerated[8]. Additionally, we reported data on secondary outcomes relevant to AD biomarkers, the SASP, cognitive function, and brain imaging[8]. As a follow-up to our original publication, we performed exploratory proteomic, lipidomic, and transcriptomic analyses on blood, CSF, and urine samples collected at baseline and post-treatment. The results provide a more comprehensive understanding of the systemic and central nervous system (CNS) effects of senolytic therapy in AD.

The heterogeneous, cell-type, and context specific phenotype of senescent cells presents a barrier in identifying appropriate biomarkers to monitor target engagement in clinical trials[9]. With this in mind, we aimed to utilize samples from the SToMP-AD pilot study to identify biomarkers that may be modulated by senolytic therapy and can be further validated by future trials on senolytics in AD and other CNS conditions. Herein, we present the baseline versus post-treatment outcomes from mass spectrometry analysis of a comprehensive list of Aß and phosphorylated tau

4

95   proteins in CSF; quantitative assays for measuring levels of cytokines and chemokines linked to

96   SASP or other hallmarks of aging measured in plasma, CSF, and urine; metabolite analysis in

97   urine; and mass spectrometry analysis of lipidomic changes in plasma and CSF. Given that

98   chronic stress is a known driver of both cellular senescence[10] and the pathologies and

99   symptomology of AD[11,12], we also measured transcriptomic changes in a chronic stress-related

100   gene profile termed the conserved transcriptional response to adversity (CTRA) in peripheral

101   blood mononuclear cells (PBMCs). This was done to probe the therapeutic utility of senolytics to

102   address the chronic-stress drivers of AD.

103

104   **Results**

105   Study Participant Sample Availability:

106   Five individuals, aged 70-82 years old, with a clinical diagnosis of early-stage dementia

107   due to AD were enrolled in the SToMP-AD pilot study. Baseline and post-treatment samples were

108   available from all five participants for tau phosphorylation protein measures (in CSF), and

109   lipidomics measures (plasma and CSF), while four of the five participant samples were available

110   for Aß isoform analysis, urine metabolites, and CTRA transcriptomic analysis. Color coding of

111   samples matches those that are described in Table 2 of the parent publication[8], which provides

112   additional information on participant characteristics.

113   Aß and tau Biomarker Measures in CSF:

114   Baseline and post-treatment Aß42 and Aß40 levels in CSF were measured by mass

115   spectrometry and the Aß42:40 ratio was calculated for each participant as a surrogate measure

116   of amyloid deposition (**Supplementary Figure 1a-d**). No statistically significant changes were

117   observed ($P > 0.05$). Similarly, baseline and post-treatment CSF levels of differentially

118   phosphorylated tau and corresponding endogenous peptides were measured (pT153, tau 151-

119   155, pT181, tau 181-190, pS199, pS202, pT205, pS208, tau 195-210, pT217, tau 212-221,

120   pT231, tau 226-230). The phosphorylated tau occupancy at different tau residues (pT111/T111,

5

121 pT153/T153, pT181/T181, pS199/S199, pT205/T205, pS208/S208, pT217/T217, pT231/T231),

122 as well as the levels of microtubule binding region (MTBR) for tau 212-221 (MTBR-tau212-221)

123 and tau 243-254 (MTBR-tau243-254, an indicator of tau tangles[13]) displayed no statistically

124 significant changes across time points (**Supplementary Figure 2 a-j** and **Supplementary Table**

125 **1**).

126 <u>Baseline ADRD Biomarkers Associated with Cerebrospinal Fluid Concentrations of Dasatinib:</u>

127   We observed a non-significant trend for increased levels of D into the CSF by individuals

128 with higher baseline CSF NfL concentrations, a marker of neurodegeneration[14] (R^2 = 0.7373; *P* =

129 0.0624; **Figure 1**). There was no correlation between CSF levels of D and measures of Aß or tau

130 as indicated by *P* > 0.05 for all analytes assessed.

131 <u>Senescence Associated Secretory Factors in Plasma, CSF, and Urine:</u>

132   Baseline to post-treatment paired samples t-tests revealed statistically significant

133 increases in four proteins analyzed from plasma, CSF and urine samples by multiplex protein

134 analysis. Though these outcomes would not have survived corrections for multiple comparisons,

135 there were significant post-treatment increases in the following multifunctional biofluid proteins:

136 plasma fractalkine and MMP-7, and CSF IL-6; other analytes that displayed trends toward change

137 at *P* < 0.1 were plasma eotaxin and VEGF (**Figure 2 and Supplementary Table 2**)**.**

138 <u>Metabolic Analysis in Urine Samples:</u>

139   Thirteen of the seventeen urinary amino acid and related metabolites measured via mass

140 spectrometry were detectable in baseline and posttreatment samples from 4 of the 5 study

141 participants, as a paired sample was not available at baseline for one of the participants. Baseline

142 to post-treatment paired samples t-tests showed no statistically significant differences in any of

143 the metabolites across time points (**Supplementary Table 3)**. Sulpiride, glutamine, glutamic acid,

144 and nicotinic acid were excluded from analyses as urinary concentration of these metabolites was

145 below the limit of quantitation (0.1 μM).

146 <u>Lipidomics Analysis in Plasma and CSF:</u>

147   MetaboAnalyst unsupervised metadata analysis on plasma lipidomics data using all 194

148   detected lipid species revealed that among all factors assessed (pre/post senolytic treatment,

149   biological sex, subject, age, and pre/post MoCA scores), biological sex had the strongest impact

150   on the circulating lipidome, followed by senolytic treatment (**Supplementary Figure 3a**). Total

151   protein content in both plasma and CSF was stable across timepoints (**Supplementary Figure**

152   **3b**). Previous metadata analysis had revealed that sex separation was largely driven by principal

153   component 1 (PC1: 33%) (**Supplementary Figure 3c**). Subsequent analyses were performed

154   following MetaboAnalyst paired one factor module using transformed and scaled lipid mass levels

155   expressed relative to plasma total protein content for both time points (**Supplementary Figure**

156   **3c**). Principal component analysis (PCA) 3D scatter-plotting revealed an evident separation

157   between baseline and post-treatment sample clusters, indicating that senolytic treatment had a

158   notable impact on the circulating lipidome as a whole (**Figure 3a**). This separation was primarily

159   driven by PC2 and PC3 (27% and 15.8%, respectively) (**Figure 3a**).

160   Paired comparisons between baseline and post-treatment plasma samples at the lipid

161   class level revealed that out of the 11 lipid classes analyzed, three classes were significantly

162   altered post-treatment when applying an unadjusted $P < 0.05$ cut-off (**Figure 3b**). These included

163   phosphatidylcholine (PC), the most abundant phospholipid in circulation and major constituent of

164   lipoprotein membranes, which decreased post-treatment by 17% ($P= 0.017$), a biologically

165   relevant amount considering that circulating PC levels are tightly regulated;

166   lysophosphatidylethanolamine (LPE), a cleavage product of the second most abundant

167   phospholipid (PE), which decreased by 22% ($P = 0.035$); and acylcarnitine an intermediate of

168   fatty acid oxidation present at very low levels in circulation that was decreased by 16% ($P = 0.004$).

169   The low acylcarnitine levels in circulation is consistent with previous reports and with the fact that

170   in plasma there are very few cell-free mitochondria or peroxisomes, the sites where acylcarnitines

171   are produced and reside. Finally, lysophosphatidylcholine (LPC), the most abundant lysolipid in

172   the circulation associated with inflammation, apoptosis, oxidative stress, and atherosclerosis[15-19],

173   displayed a 24% decreasing trend (P = 0.059) (**Figure 3b**).

174   Paired comparisons between baseline and post-treatment plasma samples at the lipid

175   species level revealed nine differentially abundant lipid species (DALs) when applying an

176   unadjusted P < 0.05 cut-off, all decreased post-treatment (**Figure 3c**). More than half of these

177   DALs were PC species of high, medium, or low abundance, including both diacyl and

178   plasmalogen species (**Figure 3d**). Additional DALs included the second most abundant LPC

179   species (18:2), which was significantly reduced by 35%, and the fourth most abundant

180   acylcarnitine species (14:2) (**Figure 3d**).

181   It is important to note that if samples are normalized to plasma volume, no separation is

182   observed by PCA (**Supplementary Figure 4a**), presumably due to the higher intrinsic

183   variability/noise associated with normalizing analytic results to sample volume. It is also worth

184   mentioning that when normalized to plasma volume, only one class was significantly altered by

185   treatment: triacylglyceride (TAG), which was increased post-treatment by 23% (**Supplementary**

186   **Figure 4b**; P = 0.022). These results are consistent with those obtained via lipid panel lab testing,

187   which are also expressed by volume, where a 28% post-treatment increasing trend was observed

188   (P = 0.064) as previously reported[8]. Additional analysis at the lipid subclass level revealed that

189   long-chain fatty acyl-containing TAGs were significantly increased (**Supplementary Figure 4c**).

190   Moreover, consistent with the above-described protein content-based results, LPC also tended to

191   decrease when normalizing to volume (**Supplementary Figure 4b**; P = 0.066). Lipid subclass

192   analyses revealed that long-chain fatty acyl-containing LPCs tended to decrease

193   (**Supplementary Figure 4d**). Finally, the vast majority of the volume-normalized DALs (4 out of

194   5) were TAG species, which increased post-treatment (**Figure 4e-f**).

195   Lastly, unsupervised dimensionality reduction (PCA) of CSF lipidomics data using all 79

196   detected lipid species normalized to total protein content revealed no separation between

197   baseline and post-treatment samples (**Supplementary Figure 5a**), implying a lack of global

198   senolytic effect at the whole CSF lipidome level. At the lipid class level, paired comparisons

199   revealed that none of the nine lipid classes assessed in the CSF were significantly altered post-

200   treatment. At the lipid species level, paired comparisons revealed five DALs when applying an

201   unadjusted $P < 0.05$ cut-off, including the second most abundant LPC species (16:1) in the CSF

202   that was reduced by 43% post-treatment (**Supplementary Figure 5c-d**; $P = 0.014$), the largest

203   effect observed by magnitude. Notably, this same LPC species came up as the most important

204   feature on a partial least squares-discriminant analysis (PLS-DA), a supervised dimensionality

205   reduction method that was able to largely separate baseline and post-treatment samples

206   (**Supplementary Figure 5b**). The other four DALs that were significantly increased post-

207   treatment included two PC species that were increased by 16% (D16:0-16:0, the second most

208   abundant PC species in CSF) and 21% (D16:1-16:0/D14:1-18:0, a medium abundant PC species)

209   post-treatment (**Supplementary Figure 5c-d**). When CSF lipidomics data were normalized to

210   volume content, none of lipid classes nor species were significantly altered. Only one species

211   (LPC 16:1) tended to change post-treatment (41% decrease, $P = 0.080$). The decrease of LPC

212   16:1 in the CSF, which reached significance when normalized to protein content as mentioned

213   above, was reminiscent and consistent with the decreases observed on other lysophospholipid

214   species in circulation.

215   Effects of Senolytic Therapy on a Transcriptomic Stress Profile:

216   Transcriptomic analysis of the PBMC samples revealed baseline to post-treatment

217   downregulation of seven of the 19 inflammatory related genes included in the Conserved

218   Transcriptional Response to Adversity (CTRA) transcriptomic stress profile; *FOSB*, *PTGS2*, *IL8*,

219   *FOS*, *IL1β*, *JUNB*, and *JUN* ($P < 0.05$; **Figure 4, Supplementary Table 4**). No significant

220   differences were seen between time points for genes within the Type I interferon or antibody

221   synthesis categories, though *IFI27L1, IFITM1,* and *IFITM4P* showed trends toward an increase

222   ($P = 0.058$; $P = 0.110$; $P = 0.110$, respectively) (**Supplementary Table 4**).

223

Discussion

In the last few years, senolytics have been translated from rodent studies to early-stage clinical trials[20]. Given the recent emergence of this therapeutic strategy, the methodology to reliably identify senescent cell presence, clearance, and the related clinical efficacy is still under development. Here we used biofluids from the first in human senolytic pilot for AD to quantify various types of analytes across multiple accessible biofluids (plasma, CSF, and urine) with the goal of determining which may be most useful and informative for exploration in future trials. Overall, no differences were detected between baseline and post-treatment in assessments for ADRD Aß and tau biomarkers, but we observed a potentially interesting trend between baseline NfL protein levels, a marker of neurodegeneration[21], and post-treatment D levels in the CSF. We also observed biofluid-specific changes in treatment response with blood analytes showing the greatest promise. Of particular interest were observed significant and/or strong trends for several blood SASP factors, lipids, and CTRA measures. These data will help direct senescence biomarker/gerodiagnostic development and refinement that can be used as a guide for outcome measures to be included in future trials.

To obtain a comprehensive analysis of ADRD biomarkers within our sample population before and after senolytic therapy, we analyzed levels of Aß and phosphorylated tau protein species and fragments currently most predictive of amyloid plaques and NFT pathology[22-26]. CSF levels of Aß and phosphorylated tau, as assessed by immunoassays, correlate with AD disease state and neurodegenerative pathology, but more disease specific information can be gleaned from assessment of the specific post-translational modifications of tau[27,28]. The Aß and tau biomarkers in our small open-label trial measured by mass spectrometry were unchanged from baseline to post-treatment. These results are consistent with those presented in initial SToMP-AD pilot trial publication[8], which were measured with the Simoa HD-X analyzer (Quanterix, Lexington, MA) and Fujirebio G1200 (Malvern, PA, lumipulse assay). Given the high precision and accuracy of these mass spectrometry assays, we interpret that the senolytic treatment did

10

250   not change CSF amyloid ß, multiple phospho-tau species, or MTBR-243 tau, a measure that

251   robustly correlates with tau tangles.

252   Throughout the disease course, Aß[29] and tau[30] biomarkers gradually change over many

253   years to decades, but levels (particularly of Aß) are dynamic, with previous studies demonstrating

254   that alterations in production and clearance are observable in response to a number of

255   interventions even within a short period of time (< 4 weeks)[31,32]. Unless plaque and tangle

256   pathologies are changing rapidly, significant alterations in these biomarkers may not be expected

257   in the 12-week intermittent treatment period of the pilot study. We note that it is encouraging that

258   AD biomarkers did not worsen, but remained stable, across the study duration. These data

259   indicate the intervention did not exacerbate disease, and may have a slowing effect of disease

260   progression as seen in mouse studies[1]. A longer duration study with a placebo arm is underway

261   and will help inform disease-modifying effects of senolytic therapy[33].

262   With advancing neurodegenerative disease, blood-brain barrier integrity becomes

263   compromised[34]. Elevations of NfL in serum have been linked with loss of blood-brain barrier

264   integrity in multiple sclerosis[35], but the degree to which CSF NfL is predictive of blood-brain barrier

265   integrity in AD is unclear[36,37]. The observed trend for increased levels of D in CSF in participants

266   with higher levels baseline CSF NfL highlights how factors relevant to AD severity and

267   neurodegenerative disease progression should be considered in regard to therapeutic effect and

268   efficacy within and across individuals. Understanding the implications of blood-brain barrier

269   integrity on the potential penetrance, uptake, and metabolism of senolytic compounds is a critical

270   pharmacological factor that will require further study in both basic science and clinical research

271   settings to ensure safety and efficacy in an early AD study population. Future studies with a larger

272   sample size will be necessary to determine if there is a true correlation between the concentration

273   of NfL or other ADRD biomarkers with the concentration of D in the central nervous system. Well-

274   designed pharmacokinetic/pharmacodynamic studies will be necessary to fully understand the

275   distribution and metabolism of senolytic compounds in healthy controls versus those with

276   neurodegenerative disease. Additionally, the inclusion of measures more directly informative

277   about blood-brain barrier integrity could be considered in future trials, including dynamic contrast

278   enhanced MRI (DCA-MRI) imaging analysis[38,39] or CSF biomarkers such as PDGFRß[40].

279   In our first publication reporting the results of the phase 1 senolytic trial in an early AD

280   population, we presented the effects of D+Q senolytic therapy on plasma and CSF SASP factors

281   measured by Quanterix and Lumipulse[8]. To futher investigate how senolytics affect SASP factors

282   and resolve discordance in the literature concerning result consistency across various assay

283   platforms, we employed multiplex magnetic bead immunoassays to measure a wider array of

284   cytokines, chemokines, growth factors, and proteinases in plasma, CSF, and urine samples. In

285   agreement with our initial report, the majority of protein biofluid markers remained unchanged

286   baseline to post-treatment, but we did observe three proteins which were significantly elevated

287   post-treatment (plasma MMP-7 and fractalkine; and CSF IL-6). Though elevation of cytokines is

288   generally indicative of inflammation, these proteins play critical roles in necessary and beneficial

289   immunological responses in neurodegenerative disease and senescent cell clearance. For

290   example, upregulation of fractalkine, a chemokine that dampens the pro-inflammatory state of

291   microglia and plays a role in adult neurogenesis, has been shown to reduce tau pathology and

292   neurodegeneration in an animal model[41], and elevated plasma fractalkine levels were protective

293   in a stroke population[42]. Elevated plasma IL-6 is indicative of increased inflammation and

294   associated with the progression and pathologies of Alzheimer's disease[43], but short-term

295   elevation may be indicative of positive biological effects in regard to the mechanisms of action of

296   senolytics and target engagement. A previous trial which utilized D+Q in a population with diabetic

297   kidney disease reported reduced levels of plasma IL-6 after only 3 days of senolytic treatment[44].

298   However, these measures were made from samples that were collected 11 days after the final

299   dose of medication, whereas in our study we report levels from samples collected immediately

300   after the final dose of D+Q, meaning participants had started their final drug administration cycle

301   24 hours prior to biofluid sample collection. It is reasonable to speculate that the increase in these

302 inflammatory related markers may be indicative of acute inflammatory response induced by D+Q

303 senescent cell ablation or "senolysis". Further, a few additional SASP related plasma proteins

304 revealed nonsignificant modest decreases post D+Q treatment (*e.g.*, eotaxin, MCP-1, VEGF),

305 which have been shown previously to elevated in AD[45], and negatively associated with memory

306 in MCI and AD[46]. It will be important for future trials to measure these SASP related factors at

307 multiple time points after completing D+Q to distinguish the acute versus chronic effects of

308 treatment[33] (ClinicalTrials.gov: NCT04685590). Within these samples, we previously reported

309 higher pre- to post-treatment CSF IL-6 levels as assessed by the Mesoscale Discovery U-Plex

310 Biomarker Group 1 (hu) 71-plex panel. Our data presented here indicate that IL-6 did not change

311 in plasma or urine to highlight the importance of biofluid consistency when measuring markers of

312 SASP as different cytokines changes were observed across plasma, CSF, and urine. Though

313 interpretation of these data is made difficult by the small sample size and lack of a control group

314 for comparison, these data nevertheless provide further evidence to guide future experimental

315 design and methods.

316 Urinary metabolite profiles have been linked with AD and proposed as potential

317 biomarkers for mild cognitive impairment and AD[47]. Recent studies from our group indicate the

318 utility of urine metabolomics to understand complex diseases[48]. In our study, urinary

319 metabolomics were unchanged. Although larger placebo-controlled studies are necessary, the

320 preliminary results are encouraging as no changes in urinary metabolites associated with adverse

321 events or AD pathogenesis were observed.

322 Due to the high lipid content of the brain and the critical role that lipids play in the integrity

323 and function of cell membranes, lipidomic measurements offer important insights to brain health

324 and disease processes[49]. Recent work indicates that lipid metabolism and homeostasis becomes

325 dysregulated with advancing neurodegeneration[50,51] and general lipidomic dysregulation in

326 AD[52,53], which highlights the potential utility of lipid measurements to be used as AD biomarkers.

327 Further, lipidomic dysregulation has been posed as a driver of cellular senescence and associated

328   inflammation[54,55], which make understanding the lipidome in AD important from the perspective

329   of both biomarker potential and AD driving insult to target therapeutically. Lipid expression relative

330   to total protein content is the most commonly used and preferred normalization method for

331   lipidomics studies[56-58], particularly for the assessment of lipids in plasma, where virtually all lipids

332   are bound to protein transporters (*e.g.*, albumin and lipoproteins), but in clinical settings lipid levels

333   are often normalized to sample volumes. Therefore, we conducted the analyses both ways to

334   determine the most appropriate method to detect lipidomic changes in response to senolytic

335   therapy. Despite the relatively short duration of senolytic treatment in this study, unsupervised

336   lipidomics analysis revealed global post-treatment effects on the circulating lipidome when

337   expressed relative to protein content that were of potential biological relevance. Although

338   senolytic treatment altered the circulating lipidome, the effect was relatively mild as it was no

339   longer observed when more stringent statistical methods were applied, which may reflect the

340   relatively short duration of the study intervention. When lipid levels were normalized to total

341   protein, senolytic treatment led to significant decreases in total LPE content and a major LPC

342   species in plasma. The reduction in circulating lysophospholipids observed following D+Q

343   treatment is suggestive of reduced inflammatory pathways and consistent with the obtained CTRA

344   transcriptomic results. These results are consistent with potential positive effects of senolytics on

345   a broad range of biological aging measures. Additionally, we found an increase in circulating TAG

346   when lipid concentrations were expressed relative to plasma volume. The fact that long-chain,

347   but not very long-chain containing TAG species, were altered, suggests that increased *de novo*

348   lipid synthesis may be responsible for the observed increase in TAG. In the SToMP-AD pilot

349   study, we previously reported a trend towards higher post-treatment total triglyceride levels in the

350   clinical lipid panel (P =0.064; Supplementary Table 1 of the parent trial results[8]), providing

351   complimentary evidence for plasma lipid changes. We also observed decreases per protein

352   content of total PC, the most abundant phospholipid on lipoprotein particle membranes. Taken

353   together, TAG and PC data suggest that senolytic therapy may illicit biological modifications of

354   lipid lipoprotein profiles. Finally, the observed decreases in circulating acylcarnitines point toward

355   a putative effect of senolytics on energy metabolism, specifically on fatty acid oxidation. These

356   potential changes require further validation to determine if lipidomic outcomes may be utilized as

357   sensitive biomarker indicators for senescent cell clearance in future trials.

358   Even through the short senolytic treatment did not have global effects on the CSF

359   lipidome, it led to robust decreases in a specific lysophospholipid species (LPC 16:1). These

360   results may be biologically relevant given the high abundance of this LPC species that is

361   consistent with the decreases in lysophospholipids observed in circulation and the expected anti-

362   inflammatory effects of senolytics. Taken together, our results place lipids as particularly sensitive

363   and clinically valuable markers, as consistent with preclinical studies[59,60] (for review: [61,62]).

364   Senolytics have been proposed as a potential therapeutic for chronic-stress induced

365   memory deficits[10]. The CTRA represents a transcriptomic profile activated by chronic stress that

366   is measured in circulating PBMCs[63]. Specifically, the CTRA transcriptomic pattern is defined by

367   relative upregulation of 19 inflammatory genes, and relative downregulation of 31 type-1 interferon

368   response genes and three antibody synthesis genes[63,64] as displayed in **Supplementary Table**

369   **4**. The CTRA has been proposed as a potential predictive biomarker for disease risk and

370   pathogenesis related to health conditions impacted by inflammatory and interferon response

371   alterations including cancer and heart disease[65], and may have utility as an indicator of AD

372   progression[64]. We were interested in assessing the utility of the CTRA as an outcome measure

373   relevant to senescence and senolytic response in AD. Our study identified a baseline to post-

374   treatment reduction in *FOSB, PTGS2, IL8, FOS, IL1β, JUNB*, and *JUN* expression in PBMCs.

375   Elevated levels of each of these transcripts have been associated with senescence and SASP

376   secretion[66-72], with our observed decreases suggesting downregulation of pathways involved in

377   inflammation and cell fate decisions[73,74] and provide exciting evidence for senolytic target

378   engagement, at least peripherally in this small pilot study. The consistent decrease in expression

379   across all seven of these differentially expressed inflammatory markers is encouraging from a

380 therapeutic standpoint as chronic peripheral inflammation[75,76], and even psychological stress[77], is

381 associated with AD. Our preclinical study of senolytics for AD previously reported an upregulation

382 in *IL1β* in the brain associated with NFTs that decreased with D+Q[1]. An independent preclinical

383 study also reported downregulation of *IL1β* in the brain in response to D+Q[3]. Recent publications

384 indicate that treatments with D+Q in animal models reduce markers of inflammation associated

385 with the pro-inflammatory senescence associated secretory proteins, including IL1β (as measured

386 in intestinal and adipose tissue in mouse models)[78,79], which was also reduced in our hands.

387 We also observed non-significant increases in *IFI27L1, IFITM1*, and *IFITM4P* type-1

388 interferon response genes. Given that these genes are typically down-regulated in CTRA, the

389 data provide additional support that senolytics may be positively impacting this chronic stress

390 pathway. While the gene expression findings in our study suggest that senolytics may impact the

391 CTRA, significant changes would not have survived multiple comparisons correction; our

392 preliminary findings require further replication in studies designed to assess this endpoint.

393 Additional work to better understand the CTRA transcriptomic profile in AD, in general, will be

394 necessary to understand the utility of this panel as a biomarker and to more fully understand the

395 implications of changes in these markers in response to senolytic therapy. Our team is currently

396 working on establishing these baseline measures in AD, and will assess the senolytic-associated

397 change in the larger Phase 2 SToMP-AD trial (NCT04685590)[33]. Notably, other trials of particular

398 interest in validating changes in CTRA are those focused on D+Q in treatment resistant

399 depression (NCT05838560)[80].

400 In summary, the stable baseline and post-treatment Aß and tau species measured with

401 mass spectrometry provide evidence that senolytic therapy does not exacerbate AD. These

402 findings also underscore the importance of identifying biomarkers specific to senolytic treatment

403 as AD surrogate measures are predicted to be downstream of senescent cell clearance. The

404 additional experimental measures comparing the baseline versus post-senolytic outcomes from

405   this study suggest that senolytics, D+Q, may, at least acutely, increase markers of inflammation,

406   while reducing circulating inflammatory lipid species and transcriptomic markers of the CTRA.

407   These supplementary measures provide clues that will contribute to the development of biomarker

408   panels associated with global senescent cell clearance specifically in an AD population. Pathways

409   and mechanisms by which D+Q may elicit a biologically relevant effect in persons with AD will

410   likely be better distinguished from the natural AD course by including a placebo control group and

411   longer study duration. There is immediate opportunity to confirm these biomarker findings in two

412   on-going Phase I D+Q trials in AD (ALSENLITE: NCT04785300; STAMINA: NCT05422885) and

413   one for treatment-resistant depression (NCT05838560). Using these exploratory outcomes as

414   biomarkers in the ongoing fully powered, double-blind, placebo-controlled phase 2 study (SToMP-

415   AD: NCT04685590) will better inform senolytic target engagement and therapeutic efficacy, that

416   will guide the development and study design of future senolytic studies.

417

418   **Methods**

419   Study Design:

420   The full study protocol[81], as well as the detailed results from the initial reporting of results

421   of the SToMP-AD trial, have been separately published[8]. In brief summary, five individuals with

422   early-stage AD were recruited to participate in an open-label trial which provided dasatinib (100

423   mg, Spruce, Bristol Meyers Squibb) and quercetin (1000 mg, Thorne Research) orally on an

424   intermittent dosing schedule for three months. The trial was conducted in compliance with all

425   relevant ethical regulations and the Guideline for Good Clinical Practice. D+Q were administered

426   under Investigation New Drug (IND) 143945-0006 (to N.M.). The study protocol was approved by

427   the UT Health San Antonio Institutional Review Board (IRB). All participants provided written

428   informed consent with an appropriate legally authorized representative.

429   Biospecimen Collection and Storage:

430   All plasma, CSF, and urine biospecimens utilized for these analyses were collected under

431   fasting conditions as described previously, at baseline (Visit 1) and post-treatment (Visit 9), the

432   morning of the second day of the final drug administration cycle[8]. Peripheral blood mononuclear

433   cell (PBMC) isolation was performed in BD Vacutainer CPT Mononuclear Cell Preparation (CPT)

434   Sodium Heparin tubes (Franklin Lakes, NJ) according to the manufacturer's protocol. The

435   resulting PBMCs were stored in three, 1 ml aliquots containing heat inactivated fetal bovine serum

436   (Corning, NY) with 10% dimethyl sulfoxide (Corning, NY). The PBMCs were stored overnight at -

437   80°C in a Mr. Frosty container (Nalgene, Rochester, NY) before final storage in a liquid nitrogen

438   freezer.

439   Mass Spectrometry for Amyloid and Tau Cerebrospinal Fluid Biomarkers:

440   Previously published methods were utilized to measure CSF Aß[82], tau and ptau peptides,

441   residues[22], and HJ32.11-MTBR-tau microtubule binding regions[24].

442   Inferring Blood-Brain-Barrier Integrity with Drug and Biomarker Correlation:

443   Levels of CSF NfL and Dasatinib penetrance into the CSF were assayed as described in

444   Gonzales et al., 2023. The Pearson r correlation between baseline NfL levels and post-treatment

445   D were assessed for each participant by simple linear regression.

446   Senescence Associated Secretory Factors in Plasma, Cerebrospinal Fluid, and Urine:

447   Baseline versus post-treatment levels of plasma, CSF, and urine biomarkers associated with

448   SASP were evaluated at the Facility for Geroscience Analysis (FGA) at Mayo Clinic. This

449   laboratory is part of the NIH-funded Translational Geroscience Network. Duplicate samples were

450   analyzed using either the FLEXMAP3D Machine (Luminex) or the Ella Automated Immunoassays

451   (Protein Simple, Bio-Techne) platforms with commercially available immunoassay kits (R&D

452   Systems, Bio-Techne). Based on the abundance of the targeted factors, bead region, and

453   antibody compatibility, the targets were organized into 18, 10, 6, and 5 plex plates for plasma and

454   15, 13, and 5 plex plates for urine. Proteins with very low abundance were measured using the

455   ELLA Automated Immunoassay (Protein Simple/Bio-Techne) with cartridges purchased from

456   Protein Simple/Bio-Techne. All assays were conducted according to the manufacturer's

457   instructions. Adiponectin was excluded from the 15-Plex urine panel due to compatibility issues

458   with the assay beads. Urine protein levels were normalized to creatinine levels for each participant

459   at each timepoint using commercially available kits (R&D Systems/Bio-Techne). The baseline and

460   post-treatment levels were compared using paired-sample t-tests to assess the effect of the

461   senolytic treatment, without correction for multiple comparisons. One participant was unable to

462   provide a baseline urine sample, so the associated post-treatment time point was excluded from

463   the analyses. Values below the assay's detection limit, resulting in the absence of a matching

464   paired sample, were excluded from the paired t-test analyses

465   <u>Metabolite Analysis in Urine Samples</u>:

466   A panel of 17 urinary metabolites were measured with urine samples collected at baseline

467   and post-treatment from 4 of the 5 study participants. Mass spectrometry (MS) protocols were

468   slightly modified from[83,84]. Briefly, for LC/MS/MS we utilized a Thermo Q Exactive HF-X Orbitrap

469   mass spectrometer with a Thermo Vanquish HPLC system, auto-injecting a 5 µL urine sample.

470   For chromatography, we used an Agilent ZORBAX HILIC PLUS column with a mobile phase of

471   components A (10 mM ammonium bicarbonate, 0.05% formic acid in Millipore water, pH=4.2) and

472   B (0.1% formic acid in acetonitrile), with flow rate flow rate of 0.3 mL/min. The gradient ran for 12

473   minutes. MS settings included a 4300 V spray voltage, nitrogen gas, ion transfer tubes, and

474   auxiliary heater at 320°C and 30°C, respectively. PRM mode was positive polarity. Data were

475   processed using Xcalibur Quant Browser, comparing peak areas to internal standards (A/IS ratio)

476   and a standard curve (0.01-100 µM) for concentration determination.

477   <u>Multidimensional Mass Spectrometry-Based Shotgun Lipidomics in Plasma and Cerebrospinal</u>

478   <u>Fluid</u>:

479   Total protein concentrations for plasma and CSF samples were determined using

480   bicinchoninic acid (BCA) protein assay (Thermo Fisher Scientific). Lipids were extracted by a

481   modified procedure of Bligh and Dyer extraction in the presence of internal standards, which were

482   added based on plasma or CSF volume for each sample as previously described[58]. Lipid analyses

483   was expressed and analyzed as per total protein content and sample volume. Lipids were

484   assessed using a triple-quadrupole mass spectrometer (Thermo Scientific TSQ Altis) and a

485   Quadrupole-Orbitrap™ mass spectrometer (Thermo Q Exactive™) equipped with a Nanomate

486   device (Advion Bioscience Ltd., NY, USA) as previously described[85,86]. Briefly, diluted lipid

487   extracts were directly infused into the electrospray ionization source through a Nanomate device,

488   signals were averaged over a 1-min period in the profile mode for each full scan MS spectrum.

489   For tandem MS, collision gas pressure was set at 1.0 mTorr, but the collision energy varied with

490   the classes of lipids. Similarly, a 2- to 5-min period of signal averaging in the profile mode was

491   employed for each tandem MS mass spectrum. All full and tandem MS mass spectra were

492   automatically acquired using a customized sequence subroutine operated through Xcalibur

493   software. Data processing including ion peak selection, baseline correction, data transfer, peak

494   intensity comparison, ^{13}C deisotoping, and quantitation were conducted using a custom

495   programmed Microsoft Excel macro after considering the principles of lipidomics[87]. Given our

496   small sample size and lack of statistical power to resolve putative sex-specific treatment effects,

497   paired analysis of all subjects (males + females) was performed to focus on the effects of senolytic

498   treatment in relation to the participant's baseline.

499   <u>RNA Preparation for Transcriptomic Analyses</u>:

500   To analyze participant PBMC samples for senolytic induced changes in genes included in

501   the CTRA transcriptomic profile, RNA was isolated from frozen PBMC samples using the QIAGEN

502   protocol for isolation of total RNA from PBMCs outlined with the RNeasy Mini Kit (ca. no. 74104).

503   RNA 260/280, 260/230, and RNA concentration were assessed using NanoDrop, and samples

504   were diluted to 10 ng/µl with RNAse free water. A nanoString nCounter XT CodeSet Gene

505   Expression Panel was designed specifically to measure the 53 gene CTRA transcriptomic profile

506   of these samples. Samples were prepared following the hybridization protocol assay (nCounter

507   XT). CTRA genes were assessed in RNA isolated from PBMC specimens using the nanoString

508   nCounter XT CodeSet Gene Expression Panel, custom designed to specifically measure the 53

509   genes which make up the CTRA profile. CTRA gene expression levels were normalized to the

510   following housekeeping genes: *HPRT1*, *PGK1*, *POLR2A*, and *TBP*, while *MAPT* was included as

511   negative control for differential gene expression analysis.

512   <u>Statistical Analysis</u>:

513   Baseline to post-treatment changes in plasma and CSF biomarkers were assessed using

514   multiple paired sample t-tests in GraphPad Prism version 9.4.1. Paired t-tests were two-tailed and

515   significance was determined by $P < 0.05$. Lipidomics statistical analysis was performed using the

516   MetaboAnalyst metadata table and paired one factor modules ((https://www.metaboanalyst.ca/).

517   Briefly, lipidomics datasets were transformed (cube root for plasma data expressed relative to

518   protein content and Log_{10} for all other data sets) and scaled (mean centered) so that the data

519   followed a normal distribution. Subclass analyses were performed in GraphPad Prism using

520   multiple paired t-tests. Normalized transcriptomic data were analyzed by moderated t-test

521   implemented in the limma package[88]. Each paired group was treated as a covariate in the design

522   matrix for the paired differentially expressed genes (DEG) analysis between baseline and post-

523   treatment samples. As with the data contained in the original report[8], *P* values were not corrected

524   for multiple comparisons due to the small sample size and exploratory nature of these reported

525   outcomes. Correlation was assessed with Pearson r analyses with simple linear regression.

526
527

570   **Conflict of Interest Statement**:

571   R.C.P. receives royalties from Oxford University Press and UpToDate and receives fees

572   from Medscape for educational activities. J.L.K. and T.T. are co-investigators on a patent for

573   Killing Senescent Cells and Treating Senescence-Associated Conditions Using an SRC Inhibitor

574   and a Flavonoid and a patent for Treating Cognitive Decline and Other Neurodegenerative

575   Conditions by Selectively Removing Senescent Cells from Neurological Tissue that are held by

576   Mayo Clinic with royalties paid to Mayo Clinic by Unity Biotechnologies. S.C. reports Scientific

577   Advisory Board membership for T3D Therapeutics and the Neurodegenerative Consortium, and

578   reports other from vTv Therapeutics, Cylcerion, T3D Therapeutics, and Cognito Therapeutics,

579   outside the submitted work. R.J.B. co-founded C2N Diagnostics. Washington University and has

580   equity ownership interest in C2N Diagnostics and receives royalty income based on technology

581   (stable isotope labeling kinetics, blood plasma assay, and methods of diagnosing AD with

582   phosphorylation changes) licensed by Washington University to C2N Diagnostics. R.J.B. receives

583   income from C2N Diagnostics for serving on the scientific advisory board. R.J.B. has received

584   research funding from Avid Radiopharmaceuticals, Janssen, Roche/Genentech, Eli Lilly, Eisai,

585   Biogen, AbbVie, Bristol Myers Squibb, and Novartis. M.M.G. reports personal stock in Abbvie.

586   R.C.P. reports personal fees from Roche, Genetech, Eli Lilly, and Nestle, and no personal fees

23

587 from Eisai, outside of the submitted work. M.E.O. has a patent Biosignature and Therapeutic

588 Approach for Neuronal Senescence pending.

589

590 **Data Availability Statement:**

591   The minimum dataset necessary to interpret, verify, and extend the research presented in

592 this article will be available upon request to the corresponding author. The trial was registered on

593 ClinicalTrials.gov: NCT04063124, the full study protocol[81] and primary and secondary aims of the

594 study[8] have been previously published.

595

596 **Contributions:**

597   M.M.G. and M.E.O. conceived the project, acquired funding, analyzed and interpreted

598 data, and edited and submitted the manuscript. V.R.G. recruited study participants, analyzed

599 samples, conducted experiments related to CTRA analyses, collected and analyzed data,

600 generated graphs and tables, and drafted the manuscript. J.P.P. performed assays and statistical

601 analyses relevant to lipidomics data. J.M., N.B., and Y.H. contributed to the HPLC-MS/MS data

602 acquisition, and interpretation. T.F.K. and J.J.M., collected biofluid samples. P.X. and B.Z.

603 performed statistical analyses and interpreted biofluid data. A.S. and N.R. conducted urinary

604 metabolite experiments and contributed to data acquisition and interpretation. K.S. provided

605 oversight and support for the urinary metabolite studies and contributed to urinary metabolite data

606 acquisition and interpretation. J.M.E.N., A.X., and T.T. contributed to biofluid analyses and

607 interpretation. M.L.C. performed HPLC-MS/MS study design, oversight, and analyses. A.S. and

608 N.M. provided medical oversight of the trial. S.S., S.C., R.C.P., J.L.K., and R.J.B. contributed to

609 data interpretation. All authors edited and approved the final manuscript.

References

1   Musi, N. *et al.* Tau protein aggregation is associated with cellular senescence in the brain. *Aging Cell* **17**, e12840, doi:10.1111/acel.12840 (2018).

2   Dehkordi, S. K. *et al.* Profiling senescent cells in human brains reveals neurons with CDKN2D/p19 and tau neuropathology. *Nature Aging* **1**, 1107-1116, doi:10.1038/s43587-021-00142-3 (2021).

3   Zhang, P. *et al.* Senolytic therapy alleviates Aβ-associated oligodendrocyte progenitor cell senescence and cognitive deficits in an Alzheimer's disease model. *Nature Neuroscience* **22**, 719-728, doi:10.1038/s41593-019-0372-9 (2019).

4   Gonzales, M. M. *et al.* A geroscience motivated approach to treat Alzheimer's disease: Senolytics move to clinical trials. *Mech Ageing Dev* **200**, 111589, doi:10.1016/j.mad.2021.111589 (2021).

5   Di Micco, R., Krizhanovsky, V., Baker, D. & d'Adda di Fagagna, F. Cellular senescence in ageing: from mechanisms to therapeutic opportunities. *Nature Reviews Molecular Cell Biology* **22**, 75-95, doi:10.1038/s41580-020-00314-w (2021).

6   Krzystyniak, A. *et al.* Combination of dasatinib and quercetin improves cognitive abilities in aged male Wistar rats, alleviates inflammation and changes hippocampal synaptic plasticity and histone H3 methylation profile. *Aging (Albany NY)* **14**, 572-595, doi:10.18632/aging.203835 (2022).

7   Wang, C. *et al.* Combined use of dasatinib and quercetin alleviates overtraining-induced deficits in learning and memory through eliminating senescent cells and reducing apoptotic cells in rat hippocampus. *Behavioural Brain Research* **440**, 114260, doi:https://doi.org/10.1016/j.bbr.2022.114260 (2023).

8   Gonzales, M. M. *et al.* Senolytic therapy in mild Alzheimer's disease: a phase 1 feasibility trial. *Nature Medicine*, doi:10.1038/s41591-023-02543-w (2023).

9   Gurkar, A. U. *et al.* Spatial mapping of cellular senescence: emerging challenges and opportunities. *Nature Aging*, doi:10.1038/s43587-023-00446-6 (2023).

10   Lin, Y. F., Wang, L. Y., Chen, C. S., Li, C. C. & Hsiao, Y. H. Cellular senescence as a driver of cognitive decline triggered by chronic unpredictable stress. *Neurobiol Stress* **15**, 100341, doi:10.1016/j.ynstr.2021.100341 (2021).

11   Ennis, G. E. *et al.* Long-term cortisol measures predict Alzheimer disease risk. *Neurology* **88**, 371-378, doi:10.1212/wnl.0000000000003537 (2017).

12   Huang, C. W. *et al.* Elevated basal cortisol level predicts lower hippocampal volume and cognitive decline in Alzheimer's disease. *J Clin Neurosci* **16**, 1283-1286, doi:10.1016/j.jocn.2008.12.026 (2009).

13   Horie, K., Barthélemy, N. R., Sato, C. & Bateman, R. J. CSF tau microtubule binding region identifies tau tangle and clinical stages of Alzheimer's disease. *Brain* **144**, 515-527, doi:10.1093/brain/awaa373 (2020).

14   Dhiman, K. *et al.* Cerebrospinal fluid neurofilament light concentration predicts brain atrophy and cognition in Alzheimer's disease. *Alzheimers Dement (Amst)* **12**, e12005, doi:10.1002/dad2.12005 (2020).

15   Lauber, K. *et al.* Apoptotic Cells Induce Migration of Phagocytes via Caspase-3-Mediated Release of a Lipid Attraction Signal. *Cell* **113**, 717-730, doi:https://doi.org/10.1016/S0092-8674(03)00422-7 (2003).

654   16   Chang, M. C. *et al.* Lysophosphatidylcholine induces cytotoxicity/apoptosis and IL-8
655   production of human endothelial cells: Related mechanisms. *Oncotarget* **8**, 106177-
656   106189, doi:10.18632/oncotarget.22425 (2017).
657   17   Corrêa, R. *et al.* Lysophosphatidylcholine Induces NLRP3 Inflammasome-Mediated
658   Foam Cell Formation and Pyroptosis in Human Monocytes and Endothelial Cells. *Front*
659   *Immunol* **10**, 2927, doi:10.3389/fimmu.2019.02927 (2019).
660   18   Matsumoto, T., Kobayashi, T. & Kamata, K. Role of lysophosphatidylcholine (LPC) in
661   atherosclerosis. *Curr Med Chem* **14**, 3209-3220, doi:10.2174/092986707782793899
662   (2007).
663   19   Plemel, J. R. *et al.* Mechanisms of lysophosphatidylcholine-induced demyelination: A
664   primary lipid disrupting myelinopathy. *Glia* **66**, 327-347, doi:10.1002/glia.23245 (2018).
665   20   Kirkland, J. L. & Tchkonia, T. Senolytic drugs: from discovery to translation. *J Intern*
666   *Med* **288**, 518-536, doi:10.1111/joim.13141 (2020).
667   21   Zetterberg, H. *et al.* Association of Cerebrospinal Fluid Neurofilament Light
668   Concentration With Alzheimer Disease Progression. *JAMA Neurol* **73**, 60-67,
669   doi:10.1001/jamaneurol.2015.3037 (2016).
670   22   Barthélemy, N. R. *et al.* CSF tau phosphorylation occupancies at T217 and T205
671   represent improved biomarkers of amyloid and tau pathology in Alzheimer's disease.
672   *Nature Aging* **3**, 391-401, doi:10.1038/s43587-023-00380-7 (2023).
673   23   Brand, A. L. *et al.* The performance of plasma amyloid beta measurements in identifying
674   amyloid plaques in Alzheimer's disease: a literature review. *Alzheimer's Research &*
675   *Therapy* **14**, 195, doi:10.1186/s13195-022-01117-1 (2022).
676   24   Horie, K. *et al.* CSF MTBR-tau243 is a specific biomarker of tau tangle pathology in
677   Alzheimer's disease. *Nature Medicine* **29**, 1954-1963, doi:10.1038/s41591-023-02443-z
678   (2023).
679   25   Ashton, N. J. *et al.* Cerebrospinal fluid p-tau231 as an early indicator of emerging
680   pathology in Alzheimer's disease. *eBioMedicine* **76**, 103836,
681   doi:https://doi.org/10.1016/j.ebiom.2022.103836 (2022).
682   26   Barthélemy, N. R. *et al.* Cerebrospinal fluid phospho-tau T217 outperforms T181 as a
683   biomarker for the differential diagnosis of Alzheimer's disease and PET amyloid-positive
684   patient identification. *Alzheimer's Research & Therapy* **12**, 26, doi:10.1186/s13195-020-
685   00596-4 (2020).
686   27   Neddens, J. *et al.* Phosphorylation of different tau sites during progression of
687   Alzheimer's disease. *Acta Neuropathologica Communications* **6**, 52,
688   doi:10.1186/s40478-018-0557-6 (2018).
689   28   Barthélemy, N. R., Horie, K., Sato, C. & Bateman, R. J. Blood plasma phosphorylated-
690   tau isoforms track CNS change in Alzheimer's disease. *J Exp Med* **217**,
691   doi:10.1084/jem.20200861 (2020).
692   29   Bateman, R. J. *et al.* Clinical and Biomarker Changes in Dominantly Inherited
693   Alzheimer's Disease. *New England Journal of Medicine* **367**, 795-804,
694   doi:10.1056/NEJMoa1202753 (2012).
695   30   McDade, E. *et al.* Longitudinal cognitive and biomarker changes in dominantly inherited
696   Alzheimer disease. *Neurology* **91**, e1295-e1306,
697   doi:doi:10.1212/WNL.0000000000006277 (2018).
698   31   Pontecorvo, M. J. *et al.* Association of Donanemab Treatment With Exploratory Plasma
699   Biomarkers in Early Symptomatic Alzheimer Disease: A Secondary Analysis of the

700   TRAILBLAZER-ALZ Randomized Clinical Trial. *JAMA Neurol* **79**, 1250-1259,
701   doi:10.1001/jamaneurol.2022.3392 (2022).

702   32   Baker, L. D. *et al.* High-intensity physical activity modulates diet effects on cerebrospinal
703   amyloid-β levels in normal aging and mild cognitive impairment. *J Alzheimers Dis* **28**,
704   137-146, doi:10.3233/jad-2011-111076 (2012).

705   33   Riessland, M. & Orr, M. E. Translating the Biology of Aging into New Therapeutics for
706   Alzheimer's Disease: Senolytics. *J Prev Alzheimers Dis* **10**, 633-646,
707   doi:10.14283/jpad.2023.104 (2023).

708   34   Sweeney, M. D., Sagare, A. P. & Zlokovic, B. V. Blood-brain barrier breakdown in
709   Alzheimer disease and other neurodegenerative disorders. *Nat Rev Neurol* **14**, 133-150,
710   doi:10.1038/nrneurol.2017.188 (2018).

711   35   Uher, T. *et al.* Neurofilament levels are associated with blood-brain barrier integrity,
712   lymphocyte extravasation, and risk factors following the first demyelinating event in
713   multiple sclerosis. *Mult Scler* **27**, 220-231, doi:10.1177/1352458520912379 (2021).

714   36   Rosengren, L. E., Karlsson, J. E., Karlsson, J. O., Persson, L. I. & Wikkelsø, C. Patients
715   with amyotrophic lateral sclerosis and other neurodegenerative diseases have increased
716   levels of neurofilament protein in CSF. *J Neurochem* **67**, 2013-2018, doi:10.1046/j.1471-
717   4159.1996.67052013.x (1996).

718   37   Barro, C., Chitnis, T. & Weiner, H. L. Blood neurofilament light: a critical review of its
719   application to neurologic disease. *Ann Clin Transl Neurol* **7**, 2508-2523,
720   doi:10.1002/acn3.51234 (2020).

721   38   Kassner, A. & Thornhill, R. Measuring the integrity of the human blood-brain barrier
722   using magnetic resonance imaging. *Methods Mol Biol* **686**, 229-245, doi:10.1007/978-1-
723   60761-938-3_10 (2011).

724   39   Kala, D. *et al.* Evaluation of blood-brain barrier integrity by the analysis of dynamic
725   contrast-enhanced MRI - a comparison of quantitative and semi-quantitative methods.
726   *Physiol Res* **71**, S259-s275, doi:10.33549/physiolres.934998 (2022).

727   40   Nation, D. A. *et al.* Blood-brain barrier breakdown is an early biomarker of human
728   cognitive dysfunction. *Nat Med* **25**, 270-276, doi:10.1038/s41591-018-0297-y (2019).

729   41   Fan, Q. *et al.* Activated CX3CL1/Smad2 Signals Prevent Neuronal Loss and Alzheimer's
730   Tau Pathology-Mediated Cognitive Dysfunction. *J Neurosci* **40**, 1133-1144,
731   doi:10.1523/jneurosci.1333-19.2019 (2020).

732   42   Donohue, M. M. *et al.* Higher plasma fractalkine is associated with better 6-month
733   outcome from ischemic stroke. *Stroke* **43**, 2300-2306, doi:10.1161/strokeaha.112.657411
734   (2012).

735   43   Barreto Chang, O. L. & Maze, M. Defining the role of Interleukin-6 for the development
736   of perioperative neurocognitive disorders: Evidence from clinical and preclinical studies.
737   *Front Aging Neurosci* **14**, 1097606, doi:10.3389/fnagi.2022.1097606 (2022).

738   44   Hickson, L. J. *et al.* Senolytics decrease senescent cells in humans: Preliminary report
739   from a clinical trial of Dasatinib plus Quercetin in individuals with diabetic kidney
740   disease. *EBioMedicine* **47**, 446-456, doi:10.1016/j.ebiom.2019.08.069 (2019).

741   45   Cho, S.-J., Park, M. H., Han, C., Yoon, K. & Koh, Y. H. VEGFR2 alteration in
742   Alzheimer's disease. *Scientific Reports* **7**, 17713, doi:10.1038/s41598-017-18042-1
743   (2017).

744   46   Bettcher, B. M. *et al.* MCP-1 and eotaxin-1 selectively and negatively associate with
745   memory in MCI and Alzheimer's disease dementia phenotypes. *Alzheimer's & Dementia:*

746		*Diagnosis, Assessment & Disease Monitoring* **3**, 91-97,
747		doi:https://doi.org/10.1016/j.dadm.2016.05.004 (2016).
748	47	Yilmaz, A. *et al.* Targeted Metabolic Profiling of Urine Highlights a Potential Biomarker
749		Panel for the Diagnosis of Alzheimer's Disease and Mild Cognitive Impairment: A Pilot
750		Study. *Metabolites* **10**, doi:10.3390/metabo10090357 (2020).
751	48	Sharma, K. *et al.* Endogenous adenine mediates kidney injury in diabetic models and
752		predicts diabetic kidney disease in patients. *J Clin Invest* **133**, doi:10.1172/jci170341
753		(2023).
754	49	Yin, F. Lipid metabolism and Alzheimer's disease: clinical evidence, mechanistic link
755		and therapeutic promise. *The FEBS Journal* **290**, 1420-1453,
756		doi:https://doi.org/10.1111/febs.16344 (2023).
757	50	Kunkle, B. W. *et al.* Genetic meta-analysis of diagnosed Alzheimer's disease identifies
758		new risk loci and implicates Aβ, tau, immunity and lipid processing. *Nat Genet* **51**, 414-
759		430, doi:10.1038/s41588-019-0358-2 (2019).
760	51	Akyol, S. *et al.* Lipid Profiling of Alzheimer's Disease Brain Highlights Enrichment in
761		Glycerol(phospho)lipid, and Sphingolipid Metabolism. *Cells* **10**,
762		doi:10.3390/cells10102591 (2021).
763	52	Liu, Y. *et al.* Plasma lipidome is dysregulated in Alzheimer's disease and is associated
764		with disease risk genes. *Translational Psychiatry* **11**, 344, doi:10.1038/s41398-021-
765		01362-2 (2021).
766	53	Byeon, S. K. *et al.* Cerebrospinal fluid lipidomics for biomarkers of Alzheimer's disease.
767		*Mol Omics* **17**, 454-463, doi:10.1039/d0mo00186d (2021).
768	54	Flor, A. C., Wolfgeher, D., Wu, D. & Kron, S. J. A signature of enhanced lipid
769		metabolism, lipid peroxidation and aldehyde stress in therapy-induced senescence. *Cell*
770		*Death Discov* **3**, 17075, doi:10.1038/cddiscovery.2017.75 (2017).
771	55	Hamsanathan, S. & Gurkar, A. U. Lipids as Regulators of Cellular Senescence. *Front*
772		*Physiol* **13**, 796850, doi:10.3389/fphys.2022.796850 (2022).
773	56	Hopp, S. C. *et al.* Multi-omics analyses reveal novel effects of PLCγ2 deficiency in the
774		mouse brain. *bioRxiv*, doi:10.1101/2023.12.06.570499 (2023).
775	57	Palavicini, J. P. *et al.* The Insulin-Sensitizer Pioglitazone Remodels Adipose Tissue
776		Phospholipids in Humans. *Front Physiol* **12**, 784391, doi:10.3389/fphys.2021.784391
777		(2021).
778	58	Wang, C., Palavicini, J. P. & Han, X. Lipidomics Profiling of Myelin. *Methods Mol Biol*
779		**1791**, 37-50, doi:10.1007/978-1-4939-7862-5_4 (2018).
780	59	Wiley, C. D. *et al.* Oxylipin biosynthesis reinforces cellular senescence and allows
781		detection of senolysis. *Cell Metab* **33**, 1124-1136.e1125, doi:10.1016/j.cmet.2021.03.008
782		(2021).
783	60	Ogrodnik, M. *et al.* Obesity-Induced Cellular Senescence Drives Anxiety and Impairs
784		Neurogenesis. *Cell Metab* **29**, 1061-1077.e1068, doi:10.1016/j.cmet.2018.12.008 (2019).
785	61	Millner, A. & Atilla-Gokcumen, G. E. Lipid Players of Cellular Senescence. *Metabolites*
786		**10**, doi:10.3390/metabo10090339 (2020).
787	62	Wiley, C. D. & Campisi, J. The metabolic roots of senescence: mechanisms and
788		opportunities for intervention. *Nat Metab* **3**, 1290-1301, doi:10.1038/s42255-021-00483-
789		8 (2021).

790   63   Cole, S. W. *et al.* Loneliness, eudaimonia, and the human conserved transcriptional
791   response to adversity. *Psychoneuroendocrinology* **62**, 11-17,
792   doi:10.1016/j.psyneuen.2015.07.001 (2015).
793   64   Cole, S. W. The Conserved Transcriptional Response to Adversity. *Curr Opin Behav Sci*
794   **28**, 31-37, doi:10.1016/j.cobeha.2019.01.008 (2019).
795   65   Simons, R. L. *et al.* An index of the ratio of inflammatory to antiviral cell types mediates
796   the effects of social adversity and age on chronic illness. *Soc Sci Med* **185**, 158-165,
797   doi:10.1016/j.socscimed.2017.03.005 (2017).
798   66   Yan, Y., Ouellette, M. M., Shay, J. W. & Wright, W. E. Age-dependent alterations of c-
799   fos and growth regulation in human fibroblasts expressing the HPV16 E6 protein. *Mol*
800   *Biol Cell* **7**, 975-983, doi:10.1091/mbc.7.6.975 (1996).
801   67   Nestler, E. J. ΔFosB: a transcriptional regulator of stress and antidepressant responses.
802   *Eur J Pharmacol* **753**, 66-72, doi:10.1016/j.ejphar.2014.10.034 (2015).
803   68   Lucibello, F. C., Brüsselbach, S., Sewing, A. & Müller, R. Suppression of the growth
804   factor-mediated induction of c-fos and down-modulation of AP-1-binding activity are not
805   required for cellular senescence. *Oncogene* **8**, 1667-1672 (1993).
806   69   Gonçalves, S. *et al.* COX2 regulates senescence secretome composition and senescence
807   surveillance through PGE(2). *Cell Rep* **34**, 108860, doi:10.1016/j.celrep.2021.108860
808   (2021).
809   70   Konishi, N. *et al.* Function of JunB in transient amplifying cell senescence and
810   progression of human prostate cancer. *Clin Cancer Res* **14**, 4408-4416,
811   doi:10.1158/1078-0432.Ccr-07-4120 (2008).
812   71   Maity, P. *et al.* Persistent JunB activation in fibroblasts disrupts stem cell niche
813   interactions enforcing skin aging. *Cell Rep* **36**, 109634, doi:10.1016/j.celrep.2021.109634
814   (2021).
815   72   Shang, D., Hong, Y., Xie, W., Tu, Z. & Xu, J. Interleukin-1β Drives Cellular Senescence
816   of Rat Astrocytes Induced by Oligomerized Amyloid β Peptide and Oxidative Stress.
817   *Front Neurol* **11**, 929, doi:10.3389/fneur.2020.00929 (2020).
818   73   Shimizu, H., Mitomo, K., Watanabe, T., Okamoto, S. & Yamamoto, K. Involvement of a
819   NF-kappa B-like transcription factor in the activation of the interleukin-6 gene by
820   inflammatory lymphokines. *Mol Cell Biol* **10**, 561-568, doi:10.1128/mcb.10.2.561-
821   568.1990 (1990).
822   74   Leppä, S. & Bohmann, D. Diverse functions of JNK signaling and c-Jun in stress
823   response and apoptosis. *Oncogene* **18**, 6158-6162, doi:10.1038/sj.onc.1203173 (1999).
824   75   Peña-Bautista, C., Casas-Fernández, E., Vento, M., Baquero, M. & Cháfer-Pericás, C.
825   Stress and neurodegeneration. *Clin Chim Acta* **503**, 163-168,
826   doi:10.1016/j.cca.2020.01.019 (2020).
827   76   Mangalmurti, A. & Lukens, J. R. How neurons die in Alzheimer's disease: Implications
828   for neuroinflammation. *Curr Opin Neurobiol* **75**, 102575,
829   doi:10.1016/j.conb.2022.102575 (2022).
830   77   Kempuraj, D. *et al.* Psychological Stress-Induced Immune Response and Risk of
831   Alzheimer's Disease in Veterans from Operation Enduring Freedom and Operation Iraqi
832   Freedom. *Clin Ther* **42**, 974-982, doi:10.1016/j.clinthera.2020.02.018 (2020).
833   78   Saccon, T. D. *et al.* Senolytic Combination of Dasatinib and Quercetin Alleviates
834   Intestinal Senescence and Inflammation and Modulates the Gut Microbiome in Aged
835   Mice. *J Gerontol A Biol Sci Med Sci* **76**, 1895-1905, doi:10.1093/gerona/glab002 (2021).

836   79   Islam, M. T. *et al.* Senolytic drugs, dasatinib and quercetin, attenuate adipose tissue
837   inflammation, and ameliorate metabolic function in old age. *Aging Cell* **22**, e13767,
838   doi:10.1111/acel.13767 (2023).
839   80   Diniz, B. S. *et al.* Geroscience-Centric Perspective for Geriatric Psychiatry: Integrating
840   Aging Biology With Geriatric Mental Health Research. *Am J Geriatr Psychiatry* **32**, 1-
841   16, doi:10.1016/j.jagp.2023.09.014 (2024).
842   81   Gonzales, M. M. *et al.* Senolytic Therapy to Modulate the Progression of Alzheimer's
843   Disease (SToMP-AD): A Pilot Clinical Trial. *J Prev Alzheimers Dis* **9**, 22-29,
844   doi:10.14283/jpad.2021.62 (2022).
845   82   Zicha, S. *et al.* Comparative analytical performance of multiple plasma Aβ42 and Aβ40
846   assays and their ability to predict positron emission tomography amyloid positivity.
847   *Alzheimer's & Dementia* **19**, 956-966, doi:https://doi.org/10.1002/alz.12697 (2023).
848   83   Nicora, C. D. *et al.* Metabolite, Protein, and Lipid Extraction (MPLEx): A Method that
849   Simultaneously Inactivates Middle East Respiratory Syndrome Coronavirus and Allows
850   Analysis of Multiple Host Cell Components Following Infection. *Methods Mol Biol*
851   **2099**, 173-194, doi:10.1007/978-1-0716-0211-9_14 (2020).
852   84   Zukunft, S. *et al.* High-throughput extraction and quantification method for targeted
853   metabolomics in murine tissues. *Metabolomics* **14**, 18, doi:10.1007/s11306-017-1312-x
854   (2018).
855   85   Wang, M., Wang, C. & Han, X. Selection of internal standards for accurate quantification
856   of complex lipid species in biological extracts by electrospray ionization mass
857   spectrometry-What, how and why? *Mass Spectrom Rev* **36**, 693-714,
858   doi:10.1002/mas.21492 (2017).
859   86   Han, X., Yang, K. & Gross, R. W. Microfluidics-based electrospray ionization enhances
860   the intrasource separation of lipid classes and extends identification of individual
861   molecular species through multi-dimensional mass spectrometry: development of an
862   automated high-throughput platform for shotgun lipidomics. *Rapid Commun Mass*
863   *Spectrom* **22**, 2115-2124, doi:10.1002/rcm.3595 (2008).
864   87   Yang, K., Cheng, H., Gross, R. W. & Han, X. Automated lipid identification and
865   quantification by multidimensional mass spectrometry-based shotgun lipidomics. *Anal*
866   *Chem* **81**, 4356-4368, doi:10.1021/ac900241u (2009).
867   88   Ritchie, M. E. *et al.* limma powers differential expression analyses for RNA-sequencing
868   and microarray studies. *Nucleic Acids Res* **43**, e47, doi:10.1093/nar/gkv007 (2015).
869

Figure Legends.

871 **Figure 1.** Correlation plot of cerebrospinal fluid (CSF) dasatinib (D) *versus* neurofilament light

872 chain (NfL) levels. Post-treatment dasatinib (D) level correlation with baseline cerebrospinal fluid

873 neurofilament light chain (NfL) derived from simple linear regression. R^2 = 0.7373; *P* = 0.0624.

874

875 **Figure 2.** Inflammatory protein levels altered by dasatinib plus quercetin (D+Q) treatment

876 measured by Luminex® protein platform. **a-d**, Effect of dasatinib plus quercetin (D+Q) on plasma

877 and cerebrospinal fluid (CSF) inflammatory markers. Mean difference (95% CI): **a**, plasma

878 fractalkine, 629 (549.90 to 705.60); **b**, plasma MMP-7, 226 (0.198 to 452.90); **c**, CSF IL-6, 1.06

879 (0.500 to 1.616). Baseline to post-treatment changes were assessed using two-sided paired

880 sample t-tests, P<0.05, N = 3-5, color coded by participant. Mean difference = post-treatment -

881 baseline; 95% CI, for the post *versus* baseline mean difference. No correction for multiple

882 comparisons was made due to small sample size.

883

884 **Figure 3**: Effects of dasatinib plus quercetin (D+Q) treatment on the circulating plasma lipidome

885 normalized to total protein concentration. **a-d**, Effects of dasatinib plus quercetin (D+Q) treatment

886 on the circulating plasma lipidome normalized to total protein content**.** Plasma lipidome was

887 assessed using multidimensional mass spectrometry-based shotgun lipidomics. **a,**

888 MetaboAnalyst unsupervised PCA plot reducing all plasma lipid species data into three

889 dimensions. Baseline and post-treatment groups are color-coded in gray and orange respectively,

890 subjects are color coded to match color code assignments across all figures. **b,** All 11 lipid classes

891 assessed in plasma samples. Paired samples are connected with a line. **c**, Volcano plot

892 comparing all 194 plasma lipid species at baseline and post-treatment. **d**, Plot of the nine

893 differentially abundant lipids (DALs) lipid species significantly decreased from baseline to post-

894 treatment. Paired samples are connected with a line, each color represents a different subject

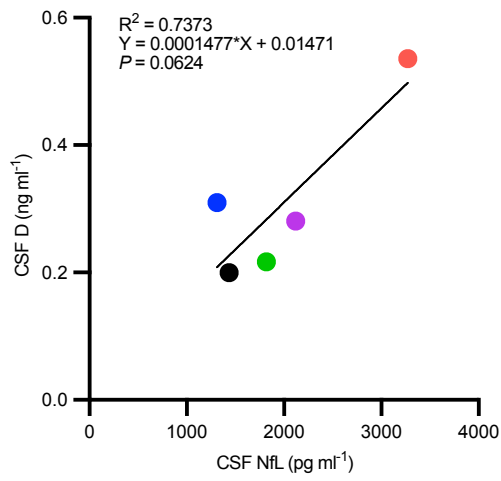895 (N=5). Only P < 0.1 are shown.

896   **Figure 4.** Baseline and post-treatment significantly differentially expressed Conserved

897   Transcriptional Response to Adversity (CTRA) gene counts in peripheral blood mononuclear cell

898   samples measured with nanoString nCounter XT CodeSet custom CTRA gene expression panel.

899   **a-g**, Effects of dasatinib plus quercetin (D+Q) on the expression of Conserved Transcriptional

900   Response to Adversity (CTRA) gene counts measured in peripheral blood mononuclear cell

901   (PBMC) samples. Seven inflammatory genes were significantly decreased post-treatment. Mean

902   difference (B-statistic): **a**, *FOSB*, -218.87 (-0.713); **b**, *PTGS2*, -377.76 (-1.177); **c**, *IL-8*, -675.93 (-

903   1.215) (**d**) *FOS*, -1579.32 (-1.669); (**e**) *IL-1B*, -152.94 (-1.922), (**f**) *JUNB*, -1267.29 (-3.546) (**g**)

904   *JUN*, -505.57 (-3.754). Baseline to post-treatment changes were assessed using two-sided paired

905   sample t-tests, *P* < 0.05, N = 4, color coded by participant. Paired baseline and post-treatment

906   measures existed for all but one of the participants (blue) for whom only a post-treatment sample

907   was collected. Mean difference = post-treatment - baseline. No correction for multiple

908   comparisons was made due to small sample size.
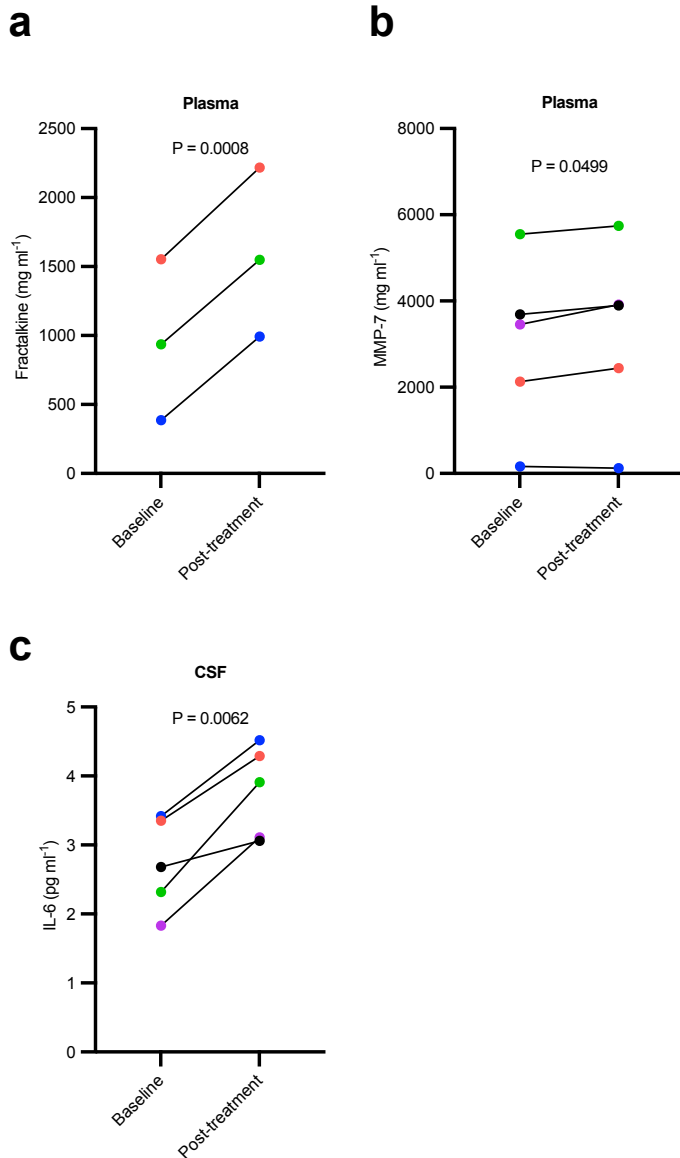
909

910

911

912

913

Figure 1. Correlation plot of cerebrospinal fluid (CSF) dasatinib (D) *versus* neurofilament light

chain (NfL) levels.

916

917

a

Plasma

P = 0.0008

Fractalkine (mg ml⁻¹)

b

Plasma

P = 0.0499

MMP-7 (mg ml⁻¹)
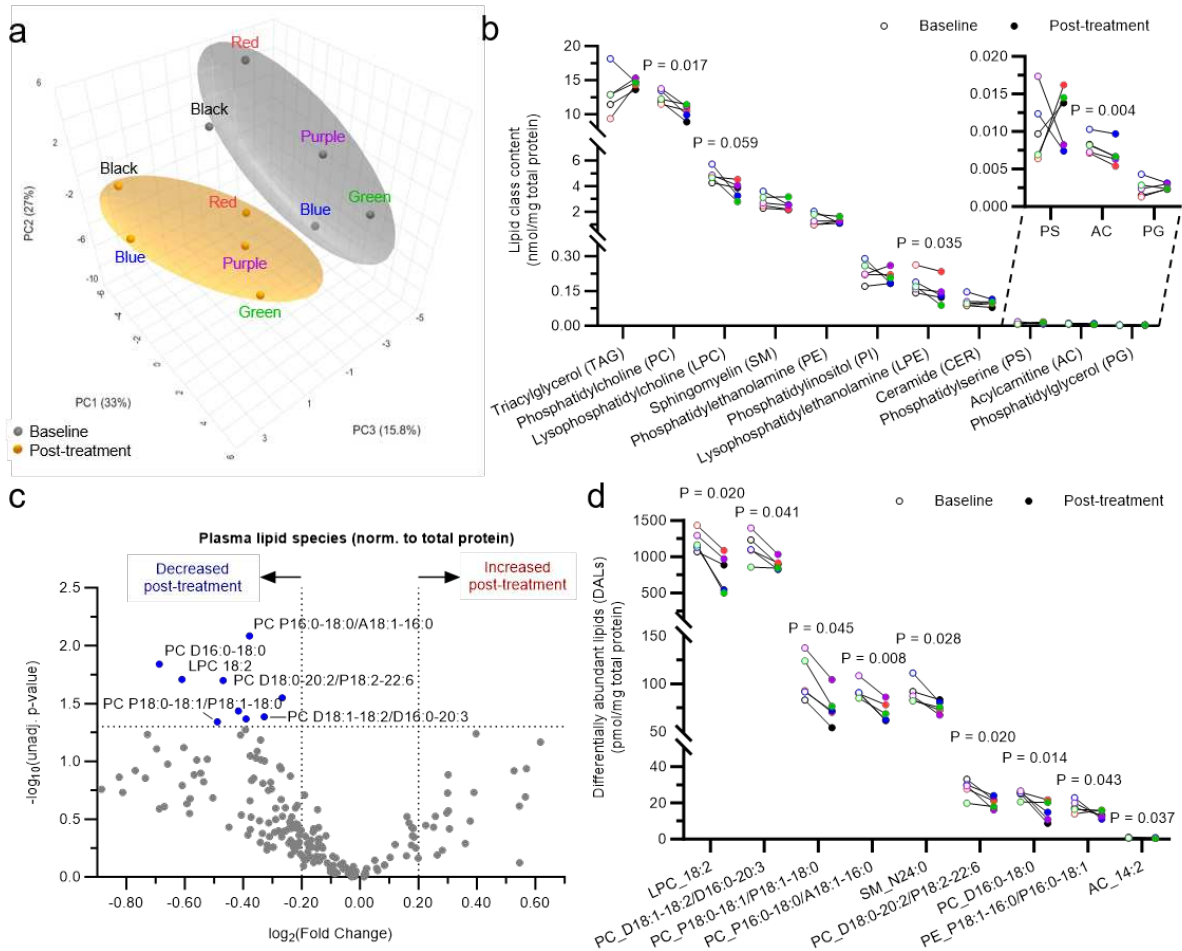
c

CSF

P = 0.0062

IL-6 (pg ml⁻¹)

918

919 **Figure 2.** Inflammatory protein levels altered by dasatinib plus quercetin (D+Q) treatment
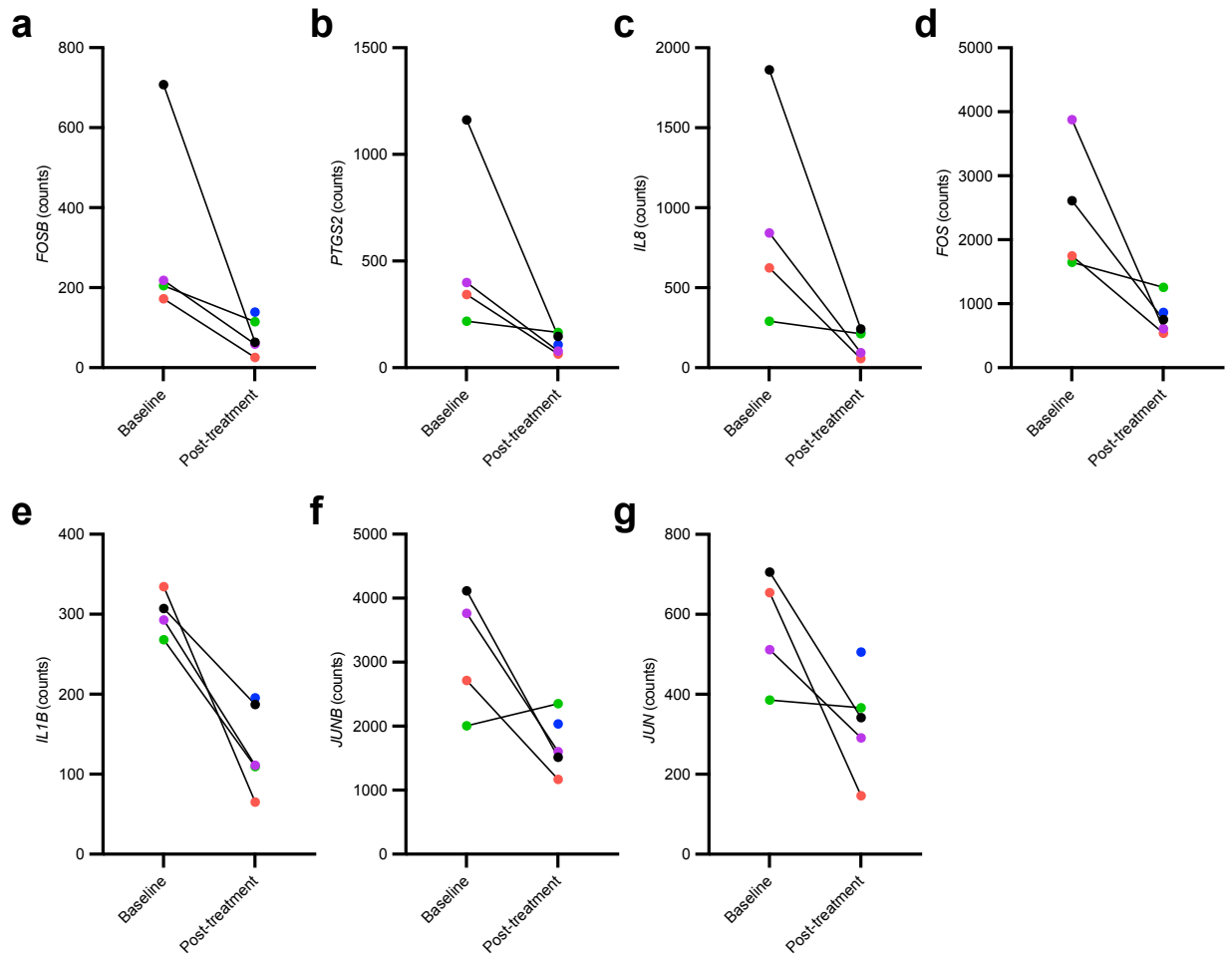
920 measured by Luminex® protein platform.

921

922

923

Figure 3: Effects of dasatinib plus quercetin (D+Q) treatment on the circulating plasma lipidome normalized to total protein concentration.

926

927
928

Figure 4. Baseline and post-treatment significantly differentially expressed Conserved Transcriptional Response to Adversity (CTRA) gene counts in peripheral blood mononuclear cell samples measured with nanoString nCounter XT CodeSet custom CTRA gene expression panel.

932

Supplementary Files

This is a list of supplementary files associated with this preprint. Click to download.

- GarbarinoetalSupplementaryTables.docx
- GarbarinoetalSupplementaryFigs.docx